PHYSICAL REVIEW B VOLUME 21, NUMBER 6 15 MARCH 1980

Impurity and temperature dependence of the electrical resistivity of dilute alloys of aluminum

Moshe Kaveh and Nathan Wiser
Department of Physics, Bar-Ilan University, Ramat-Gan, Israel
(Received 25 July 1979)

The low-temperature electrical resistivity of dilute alloys of aluminum is calculated by the variational method, based on the special properties of the electron distribution function for electron-phonon scattering. Excellent agreement is obtained with the resistivity data, both as a function of temperature and as a function of impurity concentration. The calculation is based on a multiple-OPW (orthogonalized plane-wave) description for all relevant properties of aluminum. The interference terms, resulting from the coupling between the transition probabilities for electron-phonon scattering and electron-impurity scattering, are explicitly calculated and found to be generally small. However, in the dirty limit, the interference terms become important and are responsible for the observed lack of saturation of the resistivity as a function of impurity concentration. Including the interference terms leads to agreement between theory and experiment for the resistivity over five decades of impurity concentration. Finally, the "humps" observed in the resistivity-versus-temperature curves at somewhat higher temperatures are accurately reproduced by the calculation.

I. INTRODUCTION

The most striking feature of the temperature dependence of the electrical resistivity of aluminum at low temperatures is the presence of large deviations from Matthiessen's rule (DMR). Although large DMR are observed at low temperatures for all polyvalent and noble metals,[1,2] the DMR for Al have been measured more extensively[1-30] than for any other metal because of the experimental advantages of Al. The availability of such comprehensive data is very fortunate because, from a theoretical point of view, Al is the ideal polyvalent metal to study. Al is cubic, thus simplifying all the resistivity integrals. Moreover, Ashcroft[31] has determined the detailed structure of the Fermi surface of Al, as well as the Fourier coefficients of the screened, electron-ion pseudopotential by means of an analysis of the de Haas–van Alphen data. Finally, the phonon spectrum of Al has been measured at two temperatures (80 and 300 K) and has been used to obtain[32,33] the Born–von Karman force constants out to eight sets of neighbors.

In this paper, we present the details of a calculation of the temperature dependence and impurity-concentration dependence of the electrical resistivity $\rho(T)$ for dilute alloys of Al. The overall agreement between theory and experiment for $\rho(T)$ is very good, both as a function of temperature and as a function of impurity concentration. The calculation is based on the physical ideas presented in the preceding article,[34] and the good agreement with experiment thus serves as a confirmation of these ideas. The principal new features of the calculation are the introduction of an electron distribution function that takes explicit account of the localized regions on the Fermi surface of extremely strong electron-phonon scattering and the detailed calculation of the unexpectedly large normal-scattering contribution to $\rho(T)$. Moreover, the multiple-OPW (orthogonalized plane-wave) character of Al is taken into account by introducing what we call the piecewise 2-OPW framework. This framework is shown to give a very accurate description of the electronic properties of Al, which proves to be a particularly important feature of the calculation at low temperatures.

All phases of the calculation of $\rho(T)$ are based on the known electronic and lattice properties of Al. This detailed knowledge of the properties of Al permits one to carry out realistic calculations of $\rho(T)$, including its magnitude, its temperature dependence, and its dependence on impurity concentration. The absence for Al of a host of adjustable parameters lends special significance to a comparison between theory and experiment for $\rho(T)$. Quantitative agreement with experiment implies a confirmation of the physical ideas on which the calculation of $\rho(T)$ is based, whereas discrepancies between the calculated values and the data point to shortcomings in the theory. Therefore Al provides a valuable proving ground for examining the validity of general physical concepts concerning transport in dilute alloys of polyvalent and noble metals.

In Sec. II, the general formalism is presented for the resistivity calculation and the various resistivity integrals are defined. The new electron distribution function for electron-phonon scattering is introduced in Sec. III and forms the basis for an accurate variational solution to the Boltzmann equation. In Sec. IV, the piecewise 2-OPW

framework is developed and is shown to lead to a reliable description of the properties of Al relevant to the resistivity calculation. In Sec. V, the resistivity integrands are evaluated, both for electron-phonon scattering and for electron-impurity scattering, based on the 2-OPW description of Al. Our results for the calculated resistivity of Al are given in Sec. VI and comparison is made with experiment. The interference terms are defined in Sec. VII and their contribution to the resistivity is calculated. In Sec. VIII, a discussion is given of previous work. The summary follows in Sec. IX.

II. GENERAL FORMALISM

The most convenient formalism for the calculation of the electrical resistivity is the variational formulation of the Boltzmann equation. We follow the notation of Ziman,[35] according to which the total resistivity is given by

$$\rho_{\text{tot}} = \frac{\langle\Phi|\hat{P}_{\text{tot}}|\Phi\rangle}{|\langle\Phi|X\rangle|^2}\,, \tag{2.1}$$

where $\langle\Phi|\hat{P}_{\text{tot}}|\Phi\rangle$ is the matrix element for all electron scattering processes and $\langle\Phi|X\rangle$ is the matrix element for the electric current in unit field. The total electron scattering operator $\hat{P}_{\text{tot}}$ consists of the sum

$$\hat{P}_{\text{tot}} \simeq \hat{P}_{\text{ph}} + \hat{P}_{\text{imp}}\,, \tag{2.2}$$

where the operator $\hat{P}_{\text{ph}}$ describes the scattering of electrons by phonons, and hence depends on temperature through the phonon occupation numbers, and the operator $\hat{P}_{\text{imp}}$ describes the scattering of electron by impurities, and hence depends linearly on the (dilute) concentration of impurities. Equation (2.2) is approximate because we have not included the interference term $\hat{P}_{\text{int}}$ which depends both on the temperature and on the concentration of impurities. The contribution of $\hat{P}_{\text{int}}$ will be explicitly included in Sec. VII, and shown to be generally small. The function $\Phi(\vec{K})$ describes the deviation, caused by the electric field, of the electron distribution function $f(\vec{K})$ from its equilibrium value $f_0(\vec{K})$,

$$f(\vec{K}) = f_0(\vec{K}) - \Phi(\vec{K})[\partial f_0(\vec{K})/\partial E(\vec{K})]\,. \tag{2.3}$$

The explicit expression[35] for the matrix elements is

$$\langle\Phi|\hat{P}_{\text{ph}}|\Phi\rangle = (1/k_BT)\int\int d\vec{K}_1 d\vec{K}_2[\Phi(\vec{K}_1) - \Phi(\vec{K}_2)]^2 \times \sum_\lambda \int d\vec{q}\, P_{\text{ph}}^{\vec{q}\lambda}(\vec{K}_1, \vec{K}_2; T), \tag{2.4}$$

$$\langle\Phi|\hat{P}_{\text{imp}}|\Phi\rangle = (1/2k_BT)\int\int d\vec{K}_1 d\vec{K}_2[\Phi(\vec{K}_1) - \Phi(\vec{K}_2)]^2 \times P_{\text{imp}}(\vec{K}_1, \vec{K}_2)\,,$$

where the wave vectors $\vec{K}_1$ and $\vec{K}_2$ characterize the initial and final states, respectively, of the electron being scattered by an impurity or by a phonon of wave vector $\vec{q}$, polarization λ, and frequency $\omega_\lambda(\vec{q})$. The quantity $P_{\text{imp}}(\vec{K}_1, \vec{K}_2)$ is the transition probability for electron-impurity scattering and $P_{\text{ph}}^{\vec{q}\lambda}(\vec{K}_1, \vec{K}_2; T)$ is the temperature-dependent transition probability for electron-phonon scattering via phonon destruction. Electron-phonon scattering via phonon creation contributes equally to the matrix element and has been included by multiplying the first equation of (2.4) by a factor of 2. The matrix element for the current[35] is given by

$$\langle\Phi|X\rangle = -e\int d\vec{K}\,\vec{v}(\vec{K})\Phi(\vec{K})[\partial f_0(\vec{K})/\partial E(\vec{K})] = -(e/4\pi^3\hbar)\int dS(\vec{K})\,\hat{v}(\vec{K})\Phi(\vec{K})\,, \tag{2.5}$$

where the surface integral is to be evaluated over the anisotropic Fermi surface of the metal and $\vec{v}(\vec{K})$ is the velocity of the electron in state $\vec{K}$.

The expressions for the transition probabilities are

$$P_{\text{imp}}(\vec{K}_1, \vec{K}_2) = (2\pi/\hbar)|\langle\psi_{\vec{K}_1}|\Delta\hat{W}|\psi_{\vec{K}_2}\rangle|^2 \times \delta(E(\vec{K}_2) - E(\vec{K}_1))f_0(\vec{K}_1)[1 - f_0(\vec{K}_2)]\,, \tag{2.6}$$

$$P_{\text{ph}}^{\vec{q}\lambda}(\vec{K}_1, \vec{K}_2; T) = [\pi\Omega_0/M\omega_\lambda(\vec{q})]|S_\lambda(\vec{K}_1, \vec{K}_2)|^2 \times n_{\vec{q}\lambda}\delta(E(\vec{K}_2) - E(\vec{K}_1) - \hbar\omega_\lambda(\vec{q})) \times \delta(\vec{K}_2 - \vec{K}_1 - \vec{q} - \vec{G})f_0(\vec{K}_1)[1 - f_0(\vec{K}_2)]\,,$$

where $\Delta\hat{W}$ is the pseudopotential operator due to the impurities, $\psi_{\vec{K}}(\vec{r})$ is the pseudowave function of the electron in state $\vec{K}$, Ω_0 is the volume of the unit cell, M is the ionic mass, $\vec{G}$ is a reciprocal-lattice vector, and $n_{\vec{q}\lambda}$ is the equilibrium phonon distribution function (Bose-Einstein factor). The factor $S_\lambda(\vec{K}_1, \vec{K}_2)$ is given by

$$S_\lambda(\vec{K}_1, \vec{K}_2) = \hat{\xi}_\lambda(\vec{k})\cdot\langle\psi_{\vec{K}_1}|\nabla\hat{W}|\psi_{\vec{K}_2}\rangle\,, \tag{2.7}$$

where $\hat{\xi}_\lambda(\vec{k})$ is the polarization vector for momentum transfer $\vec{k} = \vec{K}_2 - \vec{K}_1$, and $\hat{W}$ is the pseudopotential operator of the screened ions comprising the pure metal. The integrals in (2.4) may be reduced to double surface integrals over the anisotropic Fermi surface by the method so lucidly described by Ziman[35]:

$$\langle\Phi|\hat{P}_{\text{ph}}|\Phi\rangle = \frac{\Omega_0}{32\pi^5\hbar M k_BT}\int\int\left(\frac{dS(\vec{K}_1)}{v(\vec{K}_1)}\right)\left(\frac{dS(\vec{K}_2)}{v(\vec{K}_2)}\right) \times [\Phi(\vec{K}_1) - \Phi(\vec{K}_2)]^2\sum_\lambda \frac{|S_\lambda(\vec{K}_1, \vec{K}_2)|^2}{F(\omega_{\vec{q}\lambda}; T)}\,, \tag{2.8}$$

where

$$F(\omega_{\vec{q}\lambda};T) \equiv \{\exp[\hbar\omega_\lambda(\vec{q})/k_BT] - 1\} \times \{1 - \exp[-\hbar\omega_\lambda(\vec{q})/k_BT]\}, \quad (2.9)$$

and

$$\langle\Phi|\hat{P}_{\rm imp}|\Phi\rangle = \frac{c\Omega_0}{32\pi^5\hbar^3}\int\int\left(\frac{dS(\vec{K}_1)}{v(\vec{K}_1)}\right)\left(\frac{dS(\vec{K}_2)}{v(\vec{K}_2)}\right) \times [\Phi(\vec{K}_1) - \Phi(\vec{K}_2)]^2\,|\langle\psi_{\vec{K}_1}|\Delta W|\psi_{\vec{K}_2}\rangle|^2 . \quad (2.10)$$

Note that $\langle\Phi|\hat{P}_{\rm imp}|\Phi\rangle$ is independent of temperature and proportional to the concentration of impurities c, whereas $\langle\Phi|\hat{P}_{\rm ph}|\Phi\rangle$ is strongly dependent on temperature through the function $F(\omega_{\vec{q}\lambda};T)$.

This completes the presentation of the formalism. The expression for the resistivity that is embodied in (2.5)–(2.10) is perfectly general. No assumption has been made concerning the shape of the Fermi surface, the form of the electron pseudo-wave-function $\psi_{\vec{K}}(\vec{r})$, or the nonequilibrium part of the electron distribution function $\Phi(\vec{K})$.

III. VARIATIONAL SOLUTION TO BOLTZMANN EQUATION

The central problem in the calculation of the DMR is the determination of $\Phi(\vec{K})$, the solution to the Boltzmann equation in the presence of an electric field. An exact solution for $\Phi(\vec{K})$ is out of the question because of the enormous complexity of the electron-phonon scattering integral, Eqs. (2.6)–(2.8). One approach[36,37] to the problem has been to approximate the electron-phonon scattering integral to a form simple enough to permit an exact solution for $\Phi(\vec{K})$. This approach generally involves making rather drastic simplifications to the electron-phonon scattering integral, such as replacing the real metal by a model characterized by a spherical Fermi surface and single-plane-wave functions. Since the multiple-plane-wave character of the Fermi surface and of the pseudo-wave-function is essential to the description of a polyvalent metal, such model calculations cannot of course lead to quantitative agreement with experiment for $\rho(T)$. Nevertheless, exact model calculations are extremely valuable because they shed important light on the qualitative form of $\Phi(\vec{K})$.

The central result of the exact model calculations[36,37] for $\Phi(\vec{K})$, based on an idealized single-plane-wave spherical-Fermi-surface metal is that, in the absence of electron-impurity scattering, $\Phi(\vec{K})$ is dramatically reduced in the immediate vicinity of the intersections of the Fermi surface and the Brillouin-zone boundaries. Such unusual behavior for $\Phi(\vec{K})$ has been previously proposed[38] on physical grounds and is, in fact, the key to understanding the large, observed low-temperature DMR for the polyvalent and noble metals. The exact model calculations[36,37] thus confirm, at least for an idealized model, the validity of the proposed[38] functional form for $\Phi(\vec{K})$ for a polyvalent metal.

As valuable as exact model calculations are, a quantitative comparison between theory and experiment must be based on a realistic description of the metal. Therefore we calculate the electron-phonon scattering integral without approximation, including the multiple-plane-wave character of the metal. However, $\Phi(\vec{K})$ is treated approximately by means of the variational formulation of the Boltzmann equation. The variational theorem[35] states that, for the exact $\Phi(\vec{K})$, Eqs. (2.4) and (2.5) give the exact result for $\rho(T)$, whereas for any other form of $\Phi(\vec{K})$, Eqs. (2.4) and (2.5) yield a larger value for $\rho_{\rm calc}(T)$. This variational theorem is the source of the great power of the variational method. In particular, it is not necessary to prove that a newly proposed choice for $\Phi(\vec{K})$ is a more accurate solution to the Boltzmann equation than previous proposals. To establish its superiority over previous proposals, it is quite sufficient to show that the new $\Phi(\vec{K})$ leads to a lower value for $\rho_{\rm calc}(T)$.

A successful choice for $\Phi(\vec{K})$ must simulate the functional form that is expected on physical grounds. In particular, when only electron-phonon scattering is present, one must explicitly include in $\Phi(\vec{K})$ the dramatic reduction in the vicinity of the intersections of the Fermi surface and the Brillouin-zone boundaries. The details of this reduction, as well as its temperature dependence, are handled by means of a variational parameter. The following functional form[38] for $\Phi(\vec{K})$ is a convenient choice

$$\phi_{\rm ph}(\vec{K}) = [v(\vec{K})/v_F]^n\vec{v}(\vec{K})\cdot\vec{E}, \quad (3.1)$$

where v_F is the Fermi velocity over the spherical portion of the Fermi surface, $\vec{E}$ is the electric field, and the power n is determined by minimizing $\rho_{\rm calc}(T)$ at each temperature. The subscript "ph" in $\phi_{\rm ph}(\vec{K})$ denotes that this choice for $\Phi(\vec{K})$ is appropriate in the presence of electron-phonon scattering only, with no impurities present.

For the spherical portions of the Fermi surface, $v(\vec{K}) \simeq v_F$, and hence $\phi_{\rm ph}(\vec{K}) \simeq \vec{v}(\vec{K})\cdot\vec{E}$, which is the standard relaxation-time solution. However, for all polyvalent metals, for those portions of the Fermi surface near the Brillouin-zone boundaries, $v(\vec{K})$ is considerably smaller than v_F implying that $[v(\vec{K})/v_F]^n$ is negligible for large

values of n. The value of n that makes $\phi_{ph}(\vec{K})$ the optimum choice for $\Phi(\vec{K})$ is fixed automatically by the variational theorem. One would expect n to vary with temperature for the following reason. The reduction of $\phi_{ph}(\vec{K})$ from the relaxation-time solution occurs because the transition probability for electron-phonon scattering $P_{ph}^{q\lambda}(\vec{K}_1, \vec{K}_2; T)$, and hence the electron-phonon scattering integral, is very large for those portions of the Fermi surface near the Brillouin-zone boundaries. However, $P_{ph}^{q\lambda}(\vec{K}_1, \vec{K}_2; T)$ is a strong function of temperature. At low temperatures, $P_{ph}^{q\lambda}(\vec{K}_1, \vec{K}_2; T)$ is orders of magnitude larger for $\vec{K}_1$ and $\vec{K}_2$ near the Brillouin-zone boundaries than for $\vec{K}_1$ and $\vec{K}_2$ in the spherical portions of the Fermi surface. This implies that at low temperatures, n must be large to eliminate these regions of strong electron-phonon scattering from the resistivity integral. At high temperatures, however, this enormous anisotropy in electron-phonon scattering is no longer present and $P_{ph}^{q\lambda}(\vec{K}_1, \vec{K}_2; T)$ varies by only about a factor of 2–3 as $\vec{K}_1$ and $\vec{K}_2$ vary over the Fermi surface. This situation is very reminiscent of the alkali metals. For such a modest anisotropy in $P_{ph}^{q\lambda}(\vec{K}_1, \vec{K}_2; T)$, the relaxation-time solution is quite a good approximation for $\phi_{ph}(\vec{K})$, implying that $n \simeq 0$. Thus n is expected to decrease from large values at low temperatures to nearly zero at high temperatures. Such a temperature dependence for $\phi_{ph}(\vec{K})$ is confirmed by explicit calculation.

It should be emphasized that the factor $[v(\vec{K})/v_F]^n$ is introduced in (3.1) as a device to reduce $\phi_{ph}(\vec{K})$ from the relaxation-time solution in the regions of strong electron-phonon scattering. However, it is not the anisotropy of the Fermi surface that is the cause of the reduction in $\phi_{ph}(\vec{K})$. As the exact model calculations[36,37] have shown, even if one assumes a spherical Fermi surface, one still obtains that $\phi_{ph}(\vec{K})$ is nearly zero for $\vec{K}$ in the vicinity of the intersections of the Fermi surface and the Brillouin-zone boundaries. For a spherical-Fermi-surface model of a polyvalent metal, the factor $[v(\vec{K})/v_F]^n$ is of course unity for all n. Therefore, a different device would have to be used to reduce $\phi_{ph}(\vec{K})$ near the Brillouin-zone boundaries from the relaxation-time solution. One could, for example, simply set $\phi_{ph}(\vec{K})$ equal to zero for $\vec{K}$ in the region of strong electron-phonon scattering, as was discussed in the preceding paper,[34]

$$\phi_{ph}(\vec{K}) = \vec{v}(\vec{K}) \cdot \vec{E} \quad \text{for } \vec{K} \text{ not in } K^*,$$
$$\phi_{ph}(\vec{K}) = 0 \quad \text{for } \vec{K} \text{ in } K^*, \tag{3.2}$$

where the region K^* denotes the portions of the Fermi surface of very strong electron-phonon scattering for which $\phi_{ph}(\vec{K})$ is set equal to zero. The width of the region K^* would be allowed to depend on temperature and would thus play a role precisely analogous to the power n in (3.1). In each case, the presence in $\phi_{ph}(\vec{K})$ of a variational parameter that is determined automatically by the variational theorem is essential to describe the change with temperature of the functional form of $\phi_{ph}(\vec{K})$.

In addition to its well-known advantage[35] resulting from the existence of a minimization principle for $\rho_{calc}(T)$, the variational method is characterized by an additional important advantage that has not always received sufficient attention. The calculation of $\rho_{calc}(T)$, a number, is basically a much simpler problem than the calculation of $\Phi(\vec{K})$, a function. The variational method concentrates on $\rho_{calc}(T)$ and permits one to avoid almost entirely the difficult problem of calculating $\Phi(\vec{K})$. This situation has an exact analogy in the variational method of quantum mechanics[39] for solving the Schrödinger equation for the ground-state wave function $\psi_0(\vec{r})$ and ground state energy E_0. It is well known[39] that one can obtain a highly accurate value for E_0, analogous to $\rho_{calc}(T)$, even though $\psi_0(\vec{r})$, analogous to $\Phi(\vec{K})$, is known only qualitatively. The price one pays in using the variational method is that one cannot determine very accurately the detailed form of $\psi_0(\vec{r})$ or $\Phi(\vec{K})$. In fact, one obtains[39] nearly the same value for E_0 for significantly different, although similar, choices for $\psi_0(\vec{r})$. However, the reward of obtaining a highly accurate value (~1%) of E_0 or $\rho_{calc}(T)$ with relatively little effort is well worth this price of never knowing the true $\psi_0(\vec{r})$ or $\Phi(\vec{K})$.

So far, we have discussed the form of $\Phi(\vec{K})$ for pure metals, for which only electron-phonon scattering is present. For impure metals at $T = 0$ K, for which only electron-impurity scattering is present, one may use the standard relaxation-time solution

$$\phi_{imp}(\vec{K}) = \vec{v}(\vec{K}) \cdot \vec{E}. \tag{3.3}$$

This form for $\phi_{imp}(\vec{K})$ is not an exact solution to the Boltzmann equation, even for electron-impurity scattering, because of the anisotropy of the Fermi surface and the multiple-plane-wave character of the electron pseudo-wave-functions. However, Sorbello[40] has shown that the use of (3.3) for $\phi_{imp}(\vec{K})$ leads to a value for the residual resistivity ρ_0 of Al that is within a few percent of the exact value obtained by iterating the Boltzmann equation to convergence.

We are now in a position to consider the function $\Phi(\vec{K})$ appropriate to a dilute alloy, for which both electron-impurity and electron-phonon scattering are present. For an alloy, it is sufficient to take a linear combination of (3.1) and (3.3).

Thus,

$$\Phi(\vec{K}) = \phi_{imp}(\vec{K}) + \alpha\phi^*_{ph}(\vec{K}), \quad (3.4)$$

where the value of α is determined by the variational requirement that the total resistivity ρ_{tot} be minimized. Hence α depends both on the concentration of impurities c and on the temperature. The superscript * on the function $\phi^*_{ph}(\vec{K})$ denotes the following. For an alloy, the power n of $\phi_{ph}(\vec{K})$ is determined by minimizing ρ_{tot}, and thus n depends on both c and T. Therefore, for a given temperature, the function $\phi^*_{ph}(\vec{K})$ in (3.4), appropriate to the alloy, is not the same as the function $\phi_{ph}(\vec{K})$ in (3.1), appropriate to a pure metal. The value of n differs for the two cases. It is not hard to show that for very impure samples, the power n of $\phi^*_{ph}(\vec{K})$ approaches zero even at low temperatures, whereas the power n of $\phi_{ph}(\vec{K})$ is very large. Indeed, the use of $\phi_{ph}(\vec{K})$ in (3.4) would lead to significant errors in the calculation of ρ_{tot} for certain ranges of c and T.

IV. ALUMINUM

Thus far, we have described the details of the calculation of $\rho(T)$ that apply in general to any simple polyvalent metal. We now turn to the specific calculation of $\rho(T)$ for Al and describe the particular electronic and lattice properties of Al that serve as input for the calculation. These properties include (i) The Fermi surface, (ii) the pseudo-wave-function, (iii) the screened electron-ion pseudopotential matrix elements (form factor), and (iv) the phonon frequencies and polarization vectors.

A. Fermi surface

There are 15 reciprocal-lattice vectors $\vec{G}_n$ that are important for representing accurately the Fermi surface and the pseudo-wave-function of Al. These are $\vec{G}_0 = 0$, the eight $\vec{G}_n$ of length G_{111}, and the six $\vec{G}_n$ of length G_{200}. Although a complete description[31] of the Fermi surface of Al requires all 15 $\vec{G}_n$, for almost the entire Fermi surface, only two $\vec{G}_n$ are important, namely, $\vec{G}_0$ and *one* of the other 14 $\vec{G}_n$. The only exceptions to this are the small portions of the Fermi surface near the points U, K, and W on the Brillouin-zone boundary, where three $\vec{G}_n$ (near U and K) or four $\vec{G}_n$ (near W) are needed[31] to describe accurately the Fermi surface. Therefore it is sufficient to use two $\vec{G}_n$ to describe almost the entire Fermi surface, *provided* that for each point $\vec{K}$ on the Fermi surface, one uses the important nonzero $\vec{G}$ in addition to $\vec{G}_0$. We shall denote this description of the Fermi surface as the piecewise 2-OPW framework. We shall see that the piecewise 2-OPW Fermi surface closely resembles the highly accurate multiple-OPW Fermi surface.

Within the piecewise 2-OPW framework, the extended-zone-scheme Fermi surface is calculated using two normalized plane waves $|\vec{K}\rangle$ and $|\vec{K}-\vec{G}\rangle$. For each point $\vec{K}$, the most important $\vec{G}$ is clearly[41] that $\vec{G}$ that leads to the greatest distortion of the Fermi surface from the free-electron sphere. Thus, for $\vec{K}$ lying exactly on the Brillouin-zone boundary, the most important $\vec{G}$ is the one for which $\vec{K}-\vec{G}$ also lies on the Brillouin-zone boundary. However, for general $\vec{K}$, there are two factors which determine the distortion of the 2-OPW Fermi surface. One is the distance between the point $\vec{K}-\vec{G}$ and the Brillouin-zone boundary, to be denoted by $D(\vec{K}-\vec{G})$, and the second is the magnitude of $w(\vec{G})$, the matrix element of the screened electron-ion pseudopotential operator between states $|\vec{K}\rangle$ and $|\vec{K}-\vec{G}\rangle$. The distortion of the Fermi surface is greater for smaller values of $D(\vec{K}-\vec{G})$ and for larger values of $|w(\vec{G})|$. Therefore, for each point $\vec{K}$, we choose the $\vec{G}$ that minimizes the ratio $D(\vec{K}-\vec{G})/|w(\vec{G})|$.

As previously noted, the piecewise 2-OPW

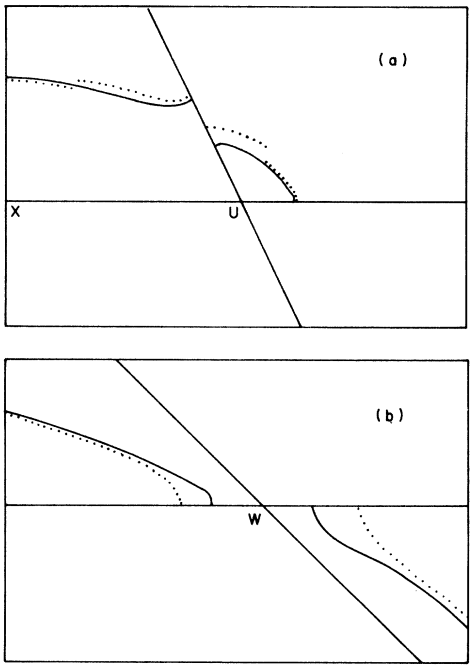

FIG. 1. Calculated Fermi surfaces for [110] cross section near the point U (a) and for [100] cross section near the point W (b). The light solid lines are the Brillouin-zone boundaries, on which are labelled the points W, U, and X. The dotted and solid curves are the piecewise 2-OPW and multiple-OPW Fermi surfaces, respectively.

Fermi surface is least accurate near the points U, K, and W of the Brillouin zone, where one needs[31] three, three, and four OPW's, respectively. In Fig. 1, we compare the piecewise 2-OPW Fermi surface with the 3-OPW Fermi surface for a [110] cross section of the Brillouin zone near the point U [Fig. 1(a)] and with the 4-OPW Fermi surface for a [100] cross section near the point W [Fig. 1(b)]. The light straight lines in the figures are the Brillouin-zone boundaries, on which are labeled the points W, U, and X. The dotted and solid curves are the piecewise 2-OPW and multiple-OPW Fermi surfaces, respectively. Note the discontinuities in the piecewise 2-OPW Fermi surface of Fig. 1(a), which indicate that for different regions of the Fermi surface, a different $\vec{G}$ minimizes the ratio $D(\vec{K}-\vec{G})/|w(\vec{G})|$. As expected, the piecewise 2-OPW framework is least accurate in the vicinity of the point W. Nevertheless, the general fit is really quite good except for the very small portion of the Fermi surface closest to W, and even there, the fit is qualitatively reasonable. We have explicitly verified that one may safely use the piecewise 2-OPW Fermi surface for the calculation of $\rho(T)$ by calculating the resistivity integrand at a few selected points on the Fermi surface near W and U and comparing the results with those obtained using the highly accurate multiple-OPW Fermi surface.

B. Pseudo-wave-functions

For the sake of consistency, we used the same piecewise 2-OPW framework to calculate the pseudo-wave-functions $\psi_{\vec{K}}(\vec{r})$. Thus,

$$\psi_{\vec{K}}(\vec{r}) = C_0(\vec{K})|\vec{K}\rangle + C_{\vec{G}}(\vec{K})|\vec{K}-\vec{G}\rangle\,, \tag{4.1}$$

where the appropriate linear combination depends of course on the value of $\vec{K}$, and hence the $\vec{K}$ dependence of $C_0(\vec{K})$ and $C_{\vec{G}}(\vec{K})$. It should be pointed out at once that the piecewise 2-OPW framework is less reliable for $\psi_{\vec{K}}(\vec{r})$ than for the Fermi surface. Indeed, its use leads to a certain error in the calculated values of $\rho(T)$ whose magnitude is hard to fix precisely. However, numerical tests that we have carried out at selected points of the resistivity integrand lead us to estimate this error at no more than 10% for any temperature.

It is readily shown[41] that for a general point on the Fermi surface, to be denoted $\vec{K}_F$, the values of $C_0(\vec{K}_F)$ and $C_{\vec{G}}(\vec{K}_F)$ are related by

$$\frac{C_{\vec{G}}(\vec{K}_F)}{C_0(\vec{K}_F)} = \frac{E_F - \hbar^2 K_F^2/2m}{w(\vec{G})}\,. \tag{4.2}$$

Equation (4.2) immediately leads to the following well-known results.[41] For $\vec{K}_F$ lying on the Brillouin-zone boundary, $E_F - \hbar^2 K_F^2/2m = \pm|w(\vec{G})|$, implying that $C_{\vec{G}}(\vec{K}_F) = \pm C_0(\vec{K}_F)$ and thus the second plane wave is very important for $\psi_{\vec{K}}(\vec{r})$. By contrast, for $\vec{K}_F$ not too near the Brillouin-zone boundary, $E_F - \hbar^2 K_F^2/2m \propto |w(\vec{G})|^2/E_F$, implying that $C_{\vec{G}}(\vec{K}_F)/C_0(\vec{K}_F) \propto |w(\vec{G})|/E_F \ll 1$. Thus, for such values of $\vec{K}_F$, the single-plane-wave approximation to $\psi_{\vec{K}}(\vec{r})$ is very good.

We now turn to the normalization of $\psi_{\vec{K}}(\vec{r})$. It is, of course, the true wave function that must be normalized to unity and not the pseudo-wave-function $\psi_{\vec{K}}(\vec{r})$. The theory of electron-phonon scattering in terms of pseudopotentials and pseudo-wave-functions was first described by Austin, Heine, and Sham,[42] who showed that the proper normalization of $\psi_{\vec{K}}(\vec{r})$ requires that

$$|C_0|^2 + |C_{\vec{G}}|^2 = 1 - \sum_c |\langle \vec{K}_F|\psi_c\rangle|^2 \equiv 1 - \Sigma\,, \tag{4.3}$$

where $|\vec{K}_F\rangle$ is a normalized plane wave of wave number K_F and $\psi_c(\vec{r})$ is an ionic core function. The core functions have been calculated and tabulated by Herman and Skillman.[43] Performing the indicated integrals of (4.3) yields for Al the value $\Sigma = 0.076$. Including the proper normalization of $\psi_{\vec{K}}(\vec{r})$ leads to a much smaller effect in $\rho(T)$ for Al than for K, for which Σ is about twice as large.[44]

C. Form factor

The form factor for electron-phonon scattering is the matrix element of the screened energy-dependent electron-ion pseudopotential operator $\hat{w}(E_F)$ between normalized plane-wave states

$$w(\vec{K}_1, \vec{K}_2; E_F) = \langle \vec{K}_1|\hat{w}(E_F)|\vec{K}_2\rangle\,. \tag{4.4}$$

Since the pseudopotential is a nonlocal energy-dependent operator $\hat{w}(E_F)$ rather than a simple function of $\vec{r}$, the matrix element $w(\vec{K}_1, \vec{K}_2; E_F)$ is, in general, a function of the six variables $\vec{K}_1$ and $\vec{K}_2$. The nonlocality of the form factor has been the object of some confusion in the literature. Thus, it is not out of place to elaborate somewhat on this point.[45] For a spherical ion, such as Al, $w(\vec{K}_1, \vec{K}_2; E_F)$ depends only on the magnitude of $\vec{K}_1$ and $\vec{K}_2$ and on the angle between them, which is conveniently given by $k = |\vec{K}_2 - \vec{K}_1|$. Thus,

$$w(\vec{K}_1, \vec{K}_2; E_F) - w(k, K_1, K_2; E_F)\,, \tag{4.5}$$

where $w(k, K_1, K_2; E_F)$ is now a function of only three variables. For the calculation of $\rho(T)$, or any transport coefficient for that matter, one requires the form factor only for both $\vec{K}_1$ and $\vec{K}_2$ lying on the Fermi surface. Therefore we denote by K_{F1} and K_{F2} the magnitude of the Fermi momentum in the directions $\hat{K}_1$ and $\hat{K}_2$, respectively, and we denote by K_F^0 the average value of K_F over

the nonspherical Fermi surface. For a spherical Fermi surface, such as for the alkali metals, K_F is constant over the Fermi surface and thus $K_{F1} = K_{F2} = K_F^0$. For a metal having a nonspherical Fermi surface, one retains the more general form $w(k, K_{F1}, K_{F2}; E_F)$. However, for a simple polyvalent metal such as Al, K_F varies very little over the Fermi surface. Indeed, the Fermi-surface calculation of Ashcroft[31] for Al has shown that the maximum deviation of K_F from K_F^0 is 3% in the [111] direction, 1% in the [100] direction, and even less in other directions. Therefore, unless the K_{F1} and K_{F2} dependences of $w(k, K_{F1}, K_{F2}; E_F)$ are unusually severe, it is quite a good approximation to replace K_{F1} and K_{F2} by K_F^0 everywhere on the Fermi surface. Thus,

$$w(k, K_1, K_2; E_F) - w(k, K_{F1}, K_{F2}; E_F) \simeq w(k, K_F^0, K_F^0; E_F). \tag{4.6}$$

Because K_F^0 and E_F are constants throughout the low-temperature calculation of $\rho(T)$, one usually writes $w(k)$ in place of $w(k, K_F^0, K_F^0; E_F)$, bearing in mind that $w(k)$ contains an explicit dependence on K_F^0 and E_F and that the maximum value of k is $k_{\max} = |\vec{K}_2 - \vec{K}_1|_{\max} = 2K_F \simeq 2K_F^0$.

The central point of the above discussion is that the form factor $w(k)$ contains *in full* the nonlocality of the pseudopotential operator, even though $w(k)$ is written for brevity as a function only of the single variable k. Nowhere has the local approximation[45] been made. The only approximation appearing in $w(k)$ is the very minor approximation given in (4.6). However, it should be added that although the form factor $w(k)$ is all that is required to calculate the transport coefficients, $w(k)$ is insufficient for calculating most other properties of the metal. For example, for the calculation of the band structure or of the phonon spectrum, one requires matrix elements of the screened pseudopotential operator for which both $\vec{K}_1$ and $\vec{K}_2$ are far from the Fermi surface. For such properties, a complete pseudopotential calculation is necessary.

The determination of $w(k)$ for the calculation of $\rho(T)$ is greatly simplified by the following considerations. At low temperatures, the significant contributions to the resistivity integral are strongly concentrated around the region $k \simeq 0$ (normal-scattering term) and the regions $k \simeq G_{111}$ and $k \simeq G_{200}$ (umklapp-scattering terms). Therefore, any form factor $w(k)$ that is accurate for the three values $k = 0$, G_{111}, G_{200} is perfectly adequate for the low-temperature calculation of $\rho(T)$. The value of $w(0)$ is known exactly[35,45] to be $-\frac{2}{3}E_F$. Moreover, the values of $w(G_{111})$ and $w(G_{200})$ have been determined experimentally for Al. An analysis[31] of the de Haas–van Alphen data yields

$$w(G_{111}) = 0.0179 \text{ Ry}, \quad w(G_{200}) = 0.0562 \text{ Ry}. \tag{4.7}$$

Therefore, knowing $w(k)$ for the important k, one is naturally led to an empirical approach to determine $w(k)$ for all $k \leq 2K_F^0$. One may use the Ashcroft[46] form factor, whose single parameter is to be chosen to yield the experimental values for $w(G_{111})$ and $w(G_{200})$. Thus

$$w(k) = \frac{-4\pi Z e^2 \cos(kR_c)}{\Omega_0 k^2 \epsilon_{\text{eff}}(k)}, \tag{4.8}$$

where R_c is the single empirical parameter in $w(k)$, Ω_0 is the atomic volume, Z is the valence, and $\epsilon_{\text{eff}}(k)$ is the effective screening function that includes,[47] in principle at least, a many-body dielectric function, the quasiparticle renormalization factor, and the irreducible vertex correction. However, it has already been shown[48] for Al that when using an empirical $w(k)$, reliance on the simple Hartree dielectric function introduces an error of only ~0.001 Ry in $w(k)$ in the vicinity of G_{111} and G_{200}. Therefore, it is certainly an adequate approximation for our purposes to replace $\epsilon_{\text{eff}}(k)$ by $\epsilon_{\text{Hartree}}(k)$. In Fig. 2, we plot $w(k)$ as a function of $k/2K_F^0$, with the experimental $w(G_{111})$ and $w(G_{200})$ indicated by the solid circles. Taking for the empirical parameter the value $R_c = 1.146$

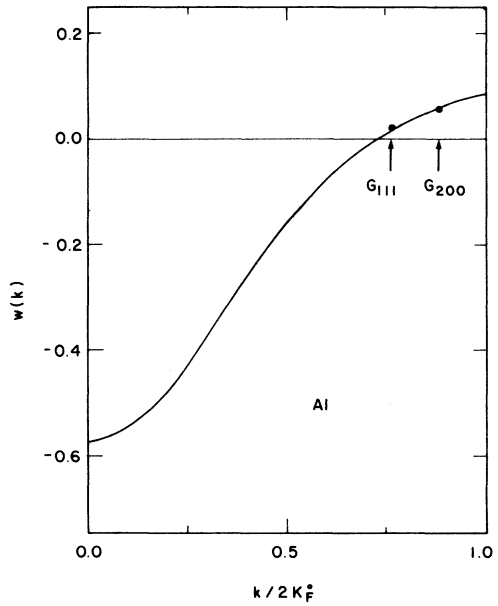

FIG. 2. Form factor $w(k)$ in Ry as a function of $k/2K_F^0$, where K_F^0 is the Fermi wave number averaged over the Fermi surface of Al. The solid circles indicate the two experimental points $w(G_{111})$ and $w(G_{200})$ and the arrows give the positions of the two reciprocal-lattice vectors that are shorter than $2K_F^0$.

a.u. leads to values for $w(G_{111})$ and $w(G_{200})$ that are within 0.003 Ry of the experimental values given in (4.7). This gives a good estimate of the maximum error present in $w(k)$ in the important region of k.

D. Phonon spectrum

The final properties of Al that enter the calculation of $\rho(T)$ are the phonon frequencies $\omega_\lambda(\vec{q})$ and polarization vectors $\hat{\xi}_\lambda(\vec{q})$ for the phonon of wave vector $\vec{q}$ and branch λ. The experimental Born–von Kármán force constants have been determined[32] for Al and their use leads to the experimental values for $\omega_\lambda(\vec{q})$ and $\hat{\xi}_\lambda(\vec{q})$ for all $\vec{q}$ and λ. However, the evaluation of the resistivity integral is greatly simplified by exploiting the following two considerations. First, for the low-temperature calculation of $\rho(T)$, one needs $\omega_\lambda(\vec{q})$ only for very small q. Therefore it is quite sufficient to neglect dispersion and assume a linear phonon spectrum. Second, for small q, the angular anisotropy of $\omega_\lambda(\vec{q})$ is very small. This is readily established by examining[41] the anisotropy factor $A = 2c_{44}/(c_{11}-c_{12})$, where c_{11}, c_{12}, and c_{44} are the three independent elastic constants of the cubic crystal. If A equals unity, there is complete elastic isotropy and the two transverse modes are degenerate.[41] Thus, the deviation of A from unity gives a quantitative measure of the elastic anisotropy. For Al, inserting the values[41] for the elastic constants yields $A-1=0.2$. To appreciate how nearly isotropic Al is, one need only contrast Al with the strongly anisotropic metal K, for which $A-1=6.6$.

In view of the small magnitude of $A-1$ for Al, it is sufficient to assume an isotropic Debye model for $\omega_\lambda(\vec{q})$ and $\hat{\xi}_\lambda(\vec{q})$, with the following values for the longitudinal and transverse velocities of sound, as obtained from the experimental force constants,[32]

$$v_L = 6.56\times 10^5 \text{ cm/sec}, \qquad v_{T1} = v_{T2} = 3.25\times 10^5 \text{ cm/sec}. \tag{4.9}$$

Explicit calculation shows that assuming complete elastic isotropy leads to a maximum error in v_L and v_T of 2% and 5%, respectively, and a maximum error in the direction of $\hat{\xi}_\lambda(\vec{q})$ of 0.0005 rad. Thus, the approximation of elastic isotropy is very appropriate to Al.

In summary, all the input data needed for the calculation of $\rho(T)$ for Al are available. In the next section, we turn to the details of the calculation.

V. RESISTIVITY INTEGRANDS

The calculation of $\rho_{\text{tot}}(T)$ requires evaluating the resistivity integrals $\langle\Phi|\hat{P}_{\text{ph}}|\Phi\rangle$ and $\langle\Phi|\hat{P}_{\text{imp}}|\Phi\rangle$, which are given by Eqs. (2.8) and (2.10). Both integrals contain the factor $[\Phi(\vec{K}_1)-\Phi(\vec{K}_2)]^2$. This factor is of utmost importance because in the present analysis, the DMR are attributed to the variation of $\Phi(\vec{K})$ with impurity concentration. We use the form (3.4) for $\Phi(\vec{K})$, with $\phi_{\text{ph}}(\vec{K})$ given by (3.1) and $\phi_{\text{imp}}(\vec{K})$ given by the relaxation-time solution $\phi_{\text{RT}}(\vec{K}) \propto \vec{v}(\vec{K})\cdot\vec{E}$, where $\vec{v}(\vec{K})$ is the velocity of the electron in state $\vec{K}$. Let us first consider the low-temperature limit, for which $\Phi(\vec{K}) \to \phi_{\text{imp}}(\vec{K}) = \phi_{\text{RT}}(\vec{K})$. One may exploit[35] the cubic symmetry of Al to average over all possible directions of the applied electric field $\vec{E}$ to obtain

$$[\Phi(\vec{K}_1)-\Phi(\vec{K}_2)]^2 \propto [\vec{v}(\vec{K}_1)-\vec{v}(\vec{K}_2)]^2 . \tag{5.1}$$

As is well known, for low temperatures, the dominant contribution to the electron-phonon integral arises from umklapp scattering for small values of $\vec{q}$, where $\vec{q}=\vec{K}_2-\vec{K}_1-\vec{G}$. This corresponds to both initial electron state $\vec{K}_1$ and final electron state $\vec{K}_2$ being in the distorted portion of the Fermi surface near its intersections with the Brillouin-zone boundaries. For such scattering events, one obtains

$$[\vec{v}(\vec{K}_1)-\vec{v}(\vec{K}_2)]^2 = (\hbar/m)^2[\hbar^2G^2/4m|w(G)|]^2q^2 . \tag{5.2}$$

If one were to ignore the multiple-plane-wave character of $\psi_{\vec{K}}(\vec{r})$ in the calculation of $\vec{v}(\vec{K})$, one would obtain the familiar single-plane-wave expression

$$[\vec{v}(\vec{K}_1)-\vec{v}(\vec{K}_2)]^2 = (\hbar/m)^2q^2 . \tag{5.3}$$

The factor in brackets, which distinguishes (5.2) from (5.3), is enormous. For example, for G_{111} for Al, one finds $[\hbar^2G^2/4m|w(G)|]^2 \sim 10^3$. In other words, the single-plane-wave approximation to (5.1) leads to an error of *three orders of magnitude* for the important region for which $\vec{K}_1$ and $\vec{K}_2$ both lie near the Brillouin-zone boundaries.

For the more general case, for which $\Phi(\vec{K}) \propto [v(\vec{K})]^n\vec{v}(\vec{K})\cdot\vec{E}$, averaging over the directions of $\vec{E}$ leads to an obvious generalization of (5.1)

$$[\Phi(\vec{K}_1)-\Phi(\vec{K}_2)]^2 \propto \{[v(\vec{K}_1)]^n\vec{v}(\vec{K}_1) - [v(\vec{K}_2)]^n\vec{v}(\vec{K}_2)\}^2 . \tag{5.4}$$

Once again, the portions of the Fermi surface near the intersections of the Brillouin-zone boundaries play a crucial role, as has already been explained in detail in Sec. III.

In the pure limit, the value of the power n in (5.4) that minimizes the resistivity integral decreases with increasing temperature, with $n_{\min}$ varying from 50 at about 20 K to 10 at about

50 K. At all temperatures, it was found that the resistivity integral as a function of n has a rather broad minimum. Varying n from $n_{\min}$ to $n_{\min} \pm 20\%$ increases the resistivity integral by less than 5%. It is satisfying to find that our choice (3.1) for $\phi_{ph}(\vec{K})$ is rather insensitive to the exact choice for $n_{\min}$. We also wished to check how sensitive the calculated resistivity is to the specific functional form (3.1). To this end, we replaced (3.1) for $\phi_{ph}(\vec{K})$ by the step function defined by (3.2) and repeated the calculation. We found that the calculated resistivity was quite close (within 10% at all temperatures) for the two choices of $\phi_{ph}(\vec{K})$, with (3.1) always giving the lower result. This lends support to our thesis that the particular functional form chosen for $\phi_{ph}(\vec{K})$ is not important. Any choice for $\phi_{ph}(\vec{K})$ that is negligible in the regions K^* of the Fermi surface and resembles $\phi_{imp}(\vec{K})$ for $\vec{K}$ not in K^* will give good results for the calculated resistivity.

The remaining factor in the integrals $\langle\phi|\hat{P}_{ph}|\phi\rangle$ and $\langle\phi|\hat{P}_{imp}|\phi\rangle$ is the transition probability for electron-phonon scattering and for electron-impurity scattering, respectively. Their evaluation is straightforward. Inserting the two-plane-wave expression for $\psi_{\vec{K}}(\vec{r})$ into the matrix element $S_\lambda(\vec{K}_1, \vec{K}_2)$, given by (2.7), yields[49]

$$S_\lambda(\vec{K}_1, \vec{K}_2) = \hat{\xi}_\lambda(\vec{k}) \cdot [\vec{k}(a_1 + a_2 + a_3 + a_4) + \vec{G}_2(a_2 + a_4) - \vec{G}_1(a_3 + a_4)] , \quad (5.5)$$

where

$$\begin{aligned} a_1 &\equiv a_1(\vec{K}_1, \vec{K}_2) \equiv C_0(\vec{K}_1) C_0(\vec{K}_2) w(k) , \\ a_2 &\equiv a_2(\vec{K}_1, \vec{K}_2) \equiv C_0(\vec{K}_1) C_{\vec{G}_2}(\vec{K}_2) w(|\vec{G}_2 + \vec{k}|) , \\ a_3 &\equiv a_3(\vec{K}_1, \vec{K}_2) \equiv C_{\vec{G}_1}(\vec{K}_1) C_0(\vec{K}_2) w(|\vec{G}_1 - \vec{k}|) , \\ a_4 &\equiv a_4(\vec{K}_1, \vec{K}_2) \equiv C_{\vec{G}_1}(\vec{K}_1) C_{\vec{G}_2}(\vec{K}_2) w(|\vec{G}_2 - \vec{G}_1 + \vec{k}|) . \end{aligned} \quad (5.6)$$

Here, $C_0(\vec{K})$ and $C_{\vec{G}}(\vec{K})$ are the coefficients of the two-plane-wave pseudo-wave-function $\psi_{\vec{K}}(\vec{r})$, given by (4.1) and (4.2), $\vec{G}_1$ and $\vec{G}_2$ are the $\vec{G}_n$ that are appropriate to $\vec{K}_1$ and $\vec{K}_2$, respectively, and $\vec{k} \equiv \vec{K}_2 - \vec{K}_1$. The arguments of the form factor are, of course, always less than $2K_F^0$. The above expression for $S_\lambda(\vec{K}_1, \vec{K}_2)$ includes the contributions of both normal scattering ($\vec{k} = \vec{q}$) and umklapp scattering ($\vec{k} = \vec{q} + \vec{G}$).

The use of two plane waves for the pseudo-wave-function leads to a form for $S_\lambda(\vec{K}_1, \vec{K}_2)$ that is significantly different from the single-plane-wave approximation. The most dramatic difference occurs for small values of q and is a matter of utmost importance at low temperatures.[49] The importance of small q scattering events is readily established by writing explicitly the sum

$$\frac{|S_L(\vec{K}_1, \vec{K}_2)|^2}{F(\omega_{\vec{q}L}^{-}; T)} + 2\frac{|S_T(\vec{K}_1, \vec{K}_2)|^2}{F(\omega_{\vec{q}T}^{-}; T)} , \quad (5.7)$$

where the factor 2 expresses the degeneracy of the transverse modes for Al. The denominator $F(\omega_{\vec{q}\lambda}^{-}; T)$, defined by (2.9), contains expressions of the form $\exp(\hbar\omega_{\vec{q}\lambda}^{-}/k_B T)$. According to (4.9), for a given q, $\omega_{qT}^{-} \simeq \frac{1}{2}\omega_{qL}^{-}$. It follows, therefore, that the second (transverse) term in (5.7) is much larger than the first (longitudinal) term, except when $S_T(\vec{K}_1, \vec{K}_2)$ exactly vanishes. This effect is particularly dramatic at low temperatures. Another important property of $F(\omega_{\vec{q}\lambda}^{-}; T)$ is that for $q \to 0$, $F(\omega_{\vec{q}\lambda}^{-}; T)$ vanishes as $[\omega_\lambda(\vec{q})]^2 \propto q^2$. By contrast, for $\hbar\omega_\lambda(\vec{q}) > k_B T$, $F(\omega_{\vec{q}\lambda}^{-}; T)$ is exponentially large. From this follows the well-known result that at low temperatures, the dominant contribution to (5.7), or equivalently to (2.8), arises from the regions of integration for which $q \to 0$.

The main point to keep in mind is that the transverse polarization and the small-q regions of the integrand are of decisive importance for electron-phonon resistivity integral. This result applies both to umklapp scattering and to normal scattering.

The resistivity integrals over the double Fermi surface were performed on the IBM 370/168 system of the Bar-Ilan University Computation Center. The multidimensional integrals were evaluated using the Harwell Library subroutine for multiple integration, based on Chebyshev polynomials. To obtain the desired 3% numerical accuracy, a different integration mesh was needed for each variable, typically ranging from 40 to 70 points per variable. However, at the lower temperatures ($\simeq$10 K), the angular integrations required a 100-point mesh. The cubic symmetry of the Fermi surface was of course exploited to reduce the range of the angular integrations.

We now turn to the electron-impurity scattering integral $\langle\phi|\hat{P}_{imp}|\phi\rangle$, given by (2.10), whose structure is much simpler than that of the electron-phonon scattering term. This simplification arises from the fact that electron-impurity scattering is not dominated by very-small-q scattering events. This is, of course, due to the absence of the phonon distribution function and its exponential temperature dependence which limits the electron-phonon scattering integral to very small q at low temperatures. However, this by no means implies that the single-plane-wave approximation is adequate for calculating the residual resistivity $\rho_0 \propto \langle\phi_{imp}|\hat{P}_{imp}|\phi_{imp}\rangle$. Indeed, Fukai[50] has shown that the single-plane-wave approximation underestimates ρ_0 by a factor of about 2 for Al and of about 3 for Pb.

This unexpected failure of the single-plane-wave approximation for ρ_0 raises a question regarding the form for the function $\phi_{\text{imp}}(\vec{K})$. The standard relaxation-time solution $\phi_{\text{RT}}(\vec{K}) \propto \vec{v}(\vec{K}) \cdot \vec{E}$ is exact[35] only if a single-plane-wave adequately represents the pseudo-wave-function. Since we have just noted that the single-plane-wave approximation is poor, one may well ask whether it is justifiable to use $\phi_{\text{RT}}(\vec{K})$ for $\phi_{\text{imp}}(\vec{K})$ in the calculation of ρ_0. Fortunately, this question has already been answered in the affirmative by the work of Sorbello.[41] He calculated ρ_0 for various different impurities in Al and found that the use of $\phi_{\text{RT}}(\vec{K})$ leads in all cases to a value of ρ_0 that is within a few percent of the exact ρ_0 obtained by an iterative solution of the Boltzmann equation. However, Sorbello pointed out[40] that $\phi_{\text{RT}}(\vec{K})$ did not give a particularly accurate representation of the electron distribution function over the Fermi surface. This is another illustration of the point we made in Sec. III, namely, that one can obtain a very accurate value for the resistivity even if one uses a distribution function that is not all that good.

It is worth emphasizing that the Sorbello calculation dealt with ρ_0 due to impurities and vacancies, for which the scattering potential is reasonably isotropic. However, if one were to consider samples for which electron-dislocation scattering makes a significant contribution to ρ_0, then the Sorbello conclusion would no longer follow. Dislocation lines are very anisotropic entities,[51] and the electron distribution function relevant to electron-dislocation scattering is significantly different[52] from $\phi_{\text{RT}}(\vec{K})$. However, the present analysis of ρ_0 is limited to impurities, vacancies, and other reasonably isotropic scattering centers, and hence we may safely use $\phi_{\text{RT}}(\vec{K})$ for $\phi_{\text{imp}}(\vec{K})$ without further discussion. In a subsequent paper, we plan to treat the interesting changes in $\rho_{\text{tot}}(T)$ that result from the presence of electron-dislocation scattering.

Since we are dealing with a low concentration of random impurities or vacancies, the structure factor is unity[35] for all $\vec{k}$ and we concentrate on the matrix element $\langle \psi_{\vec{K}_1} | \Delta\hat{w} | \psi_{\vec{K}_2} \rangle$, where $\Delta\hat{w}$ is the screened pseudopotential operator of a single scattering center. The matrix element is not a form factor because $\psi_{\vec{K}}(\vec{r})$ is a two-plane-wave pseudo-wave-function. Inserting the two-plane-wave expression for $\psi_{\vec{K}}(\vec{r})$ yields

$$\begin{aligned}\langle \psi_{\vec{K}_1} | \Delta w | \psi_{\vec{K}_2} \rangle = {} & C_0(\vec{K}_1) C_0(\vec{K}_2) \Delta w(k) \\ & + C_0(\vec{K}_1) C_{\vec{G}_2}(\vec{K}_2) \Delta w(|\vec{G}_2 + \vec{k}|) \\ & + C_{\vec{G}_1}(\vec{K}_1) C_0(\vec{K}_2) \Delta w(|\vec{G}_1 - \vec{k}|) \\ & + C_{\vec{G}_1}(\vec{K}_1) C_{\vec{G}_2}(\vec{K}_2) \Delta w(|\vec{G}_2 - \vec{G}_1 + \vec{k}|), \end{aligned} \tag{5.8}$$

where $\Delta w(k)$ is the form factor $\langle \vec{K}_1 | \Delta\hat{w} | \vec{K}_2 \rangle$ between normalized plane waves. For the simplest case of a substitutional impurity, the screened pseudopotential operator $\Delta\hat{w}$ is the bare pseudopotential operator of the impurity $\hat{w}_{\text{imp}}^{\text{bare}}$ minus the bare pseudopotential operator of the host $\hat{w}_{\text{host}}^{\text{bare}}$ (Al, in the present case), screened by the screening function of the host. One may safely neglect the slight change in electron density in going from the pure host to the dilute alloy. Using the Ashcroft[46] form of the form factor, one readily obtains

$$\Delta w(k) = w_{\text{host}}(k) \left(\frac{Z_{\text{imp}} \cos(kR_c^{\text{imp}})}{Z_{\text{host}} \cos(kR_c^{\text{host}})} - 1 \right), \tag{5.9}$$

where Z_{imp} and Z_{host} are the ionic charges of the impurity and of the host, respectively. The values for R_c^{imp} for various impurities were taken from Table I of Fukai.[50] It is clear from (5.9) that for all k, $\Delta w(k)$ is the same order of magnitude as $w_{\text{host}}(k)$. Thus, there is no qualitative difference between an impurity and a vacancy, characterized by $Z_{\text{imp}} = 0$, for which $\Delta w(k) = -w_{\text{host}}(k)$. Therefore we shall henceforth use the general term "impurity" to include either a vacancy or a substitutional impurity.

VI. RESULTS AND COMPARISON WITH EXPERIMENT

In Secs. IV and V, the parameters characterizing Al were presented and the resistivity integrals were defined in terms of these parameters. With this information, one is in a position to evaluate the integrals (2.5), (2.8), and (2.10) over the true anisotropic Fermi surface of Al to obtain numerical results for the calculated resistivity $\rho_{\text{tot}}(T)$. The quantity of physical interest is of course not the total resistivity, but rather its temperature-dependent part $\Delta\rho(T)$, which is given by

$$\Delta\rho(T) = \rho_{\text{tot}}(T) - \rho_0 . \tag{6.1}$$

Since $\Delta\rho(T)$ depends both on temperature and on ρ_0 (through its dependence on the impurity concentration), one may display the data for $\Delta\rho(T)$ as a function of T for various fixed values of ρ_0 (the usual graphs) or a function of ρ_0 for various fixed values of T (the DMR graphs).

We compare our calculated results for $\Delta\rho(T)$ for Al with detailed measurements of Papastaikoudis, Papathanasopoulos, Rocofyllou, and coworkers.[14-16,21-23] In Fig. 3, the solid curve represents the calculation and the various symbols represent the data for $\Delta\rho(T)/T^3$ for four different samples containing two different types of impurities (Ga and Ge). The values for R_c^{imp} for Ga and Ge were taken from Fukai.[50] The agreement between theory and experiment is evident from

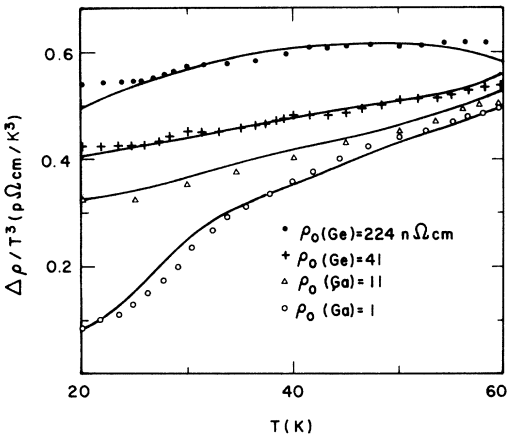

FIG. 3. Temperature dependence of $\Delta\rho/T^3$ for four different samples of Al containing two different types of impurities, Ga and Ge. The various symbols are experimental points and the solid curves give the calculated values.

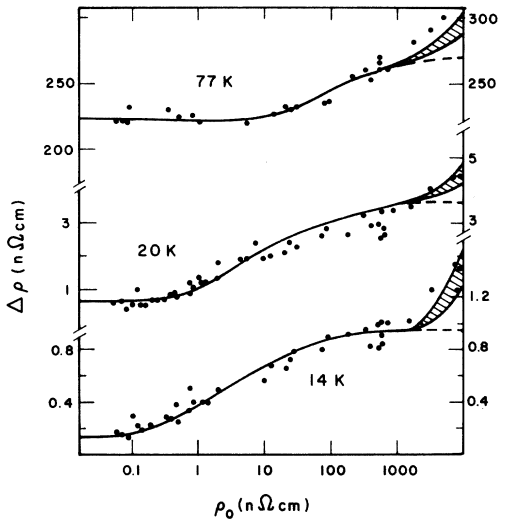

FIG. 4. Plots of $\Delta\rho$ as a function of ρ_0 for three different temperatures. The experimental points were taken from the compilation of data given in Ref. 2. The solid curves are the calculated values. The dashed lines for large ρ_0 ($\gtrsim$1000 nΩcm) represent the values for $\Delta\rho$ calculated without including the contribution of the interference terms $\Delta\rho_{\rm int}(T)$. The hatched area of each curve gives an estimate of the spread in $\Delta\rho_{\rm int}(T)$ due to the dependence on the type of impurity present.

the figure. At 20 K, the sample dependence is very marked, with $\Delta\rho(T)$ varying for different samples by a factor of 5 as ρ_0 varies from 1 to 224 nΩ cm. However, by 60 K, the $\Delta\rho(T)$ data have become almost sample independent, varying by only 20% over the same range of ρ_0. These results are in precise agreement with the theory.

A point of particular interest is that neither theory nor experiment yields power-law behavior for the temperature dependence of $\Delta\rho(T)$. Although the dirtiest sample does exhibit T^3 behavior fairly closely for $\Delta\rho(T)$ over the entire temperature range, this is clearly not the case for the purer samples. In fact, there is no reason, neither experimental nor theoretical, to expect T^3 behavior for $\Delta\rho(T)$ for all samples, as has sometimes been proposed.[1,2] Similar remarks apply equally well to the $\Delta\rho(T)$ data below 20 K, which we have discussed in an earlier publication[38] dealing with the lower-temperature regime.

There exist of course additional data[1,2] for $\Delta\rho(T)$ for Al. However, the data[14-16,21-23] of the research group of the Democritos Nuclear Research Center of Athens are unusually complete and care was taken to identify the impurity present in each sample, features which make these data particularly useful for comparison with the theory. We therefore focus our attention on the comprehensive data of the Athens group. However, it should be clear that comparing our calculated results with other data[1,2] leads to comparable agreement.

The other curves of interest are the DMR graphs, giving $\Delta\rho(T)$ as a function of ρ_0 for various fixed values of the temperature. Such curves are presented in Fig. 4 for T = 14, 20, and 77 K, for ρ_0 ranging from 0.1 to 10^4 nΩ cm. The data were taken from the compilation of Cimberle, Bobel, and Rizzuto.[2] It is convenient to discuss separately two different regimes for ρ_0. First, consider $\rho_0 < 1$ $\mu\Omega$ cm. For this regime, it is evident from Fig. 4 that the calculated curves accurately reproduce the data for all temperatures. It should be noted that the temperature range 14–77 K corresponds to a range of three orders of magnitude for $\Delta\rho(T)$. The DMR are very large at 14 K (about a factor of 6) and drop to only about 20% at 77 K. Note also that for each temperature, the observed pure-limit value for $\Delta\rho(T)$ is quantitatively given by the calculation.

For both the pure limit and the dirty limit, $\Delta\rho(T)$ is independent of the type of impurity present. However, for the intermediate regime, $\Delta\rho(T)$ does depend on the type of impurity. Since this information is not available for many of the samples reported, we arbitrarily assumed vacancy scattering for all samples, corresponding to an "impurity" with $Z_{\rm imp}=0$. This will lead to an uncertainty that approaches nearly 20% in the middle of the intermediate regime and becomes negligible as one approaches the pure and dirty limits. It is just possible that at least part of the scatter of the data in the intermediate regime is a real effect due to different impurities present in different samples. This matter deserves fur-

ther study.

We now turn to the large-ρ_0 regime, $\rho_0 > 1$ $\mu\Omega$ cm. The calculation described thus far predicts a dirty limit, characterized by saturation of $\Delta\rho(T)$ for large values of ρ_0, as given by the dashed lines in Fig. 4. By contrast, the data show no signs of saturation, continuing to rise with increasing ρ_0. This additional rise of $\Delta\rho(T)$ for $\rho_0 > 10^3$ nΩ cm is due to the interference terms $\Delta\rho_{\text{int}}(T)$, first discussed by Kagan and Zhernov.[53] Although the calculation of $\Delta\rho_{\text{int}}(T)$ for Al will be presented in Sec. VII, we here anticipate the results. The hatched curves in Fig. 4 include the contribution of $\Delta\rho_{\text{int}}(T)$ to $\Delta\rho(T)$. The calculated values for $\Delta\rho_{\text{int}}(T)$ vary with the type of impurity present by as much as a factor of 2. The width of the hatched curves thus expresses our lack of knowledge on this point.

The values for $\Delta\rho_{\text{int}}(T)$ are negligible for $\rho_0 \lesssim 1$ $\mu\Omega$ cm. For $\rho_0 = 10$ $\mu\Omega$ cm, $\Delta\rho_{\text{int}}(T)$ is about 30% of $\Delta\rho(T)$ in the dirty limit at 14 K and decreases to about 5% of $\Delta\rho(T)$ at 77 K. Thus, the magnitude of $\Delta\rho_{\text{int}}(T)$ is not particularly large at any temperature. However, without including $\Delta\rho_{\text{int}}(T)$, one cannot explain the continued rise in $\Delta\rho(T)$ in the dirty limit. We note with satisfaction that including $\Delta\rho_{\text{int}}(T)$ leads to close agreement between theory and experiment for all temperatures over five orders of magnitude for ρ_0.

A third type of graph that has frequently been plotted is that shown in Fig. 5. One introduces $\Delta(T)$, defined as the deviation from Matthiessen's rule,

$$\Delta(T) = \rho_{\text{tot}}(T) - \rho_0 - \rho_{\text{pure}}(T) = \Delta\rho(T) - \rho_{\text{pure}}(T), \tag{6.2}$$

where $\rho_{\text{pure}}(T)$ is the ideal resistance in the absence of impurities. The graph gives $\Delta(T)/\rho_0$ as a function of temperature. The solid curves represent the calculation and the various symbols represent the data for four different concentrations of Mg impurities in Al. Once again, the agreement between theory and experiment is evident for all four curves. To illustrate that the theory also reproduces the data of workers other than the Athens group, we used the data of Seth and Woods[5] for $\rho_0 = 681$ nΩ cm. As before, the solid curves include the contribution of $\Delta\rho_{\text{int}}(T)$, whereas the dashed curves give the results without the interference terms. It is seen that $\Delta\rho_{\text{int}}(T)$ is significant only for the more impure samples and only for higher temperatures.

The most characteristic feature[1] of the curves in Fig. 5 is the so-called "hump," a maximum in $\Delta(T)$ that occurs at a temperature T_{max}. The value for T_{max} is about 0.1–0.2 of the Debye temperature

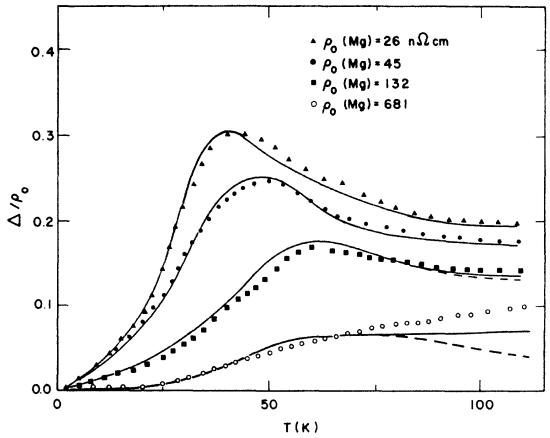

FIG. 5. Temperature dependence of $\Delta(T)/\rho_0$ for four different concentrations of Mg impurities in Al. Note the characteristic "hump", the observed maximum in $\Delta(T)$, for each sample, except the most impure one. The various symbols are the experimental points. The solid curves give the calculated values. The dashed lines for the two more impure samples at high temperatures represent the values of $\Delta(T)$ calculated without including the interference terms.

and increases slowly with increasing impurity concentration. The Athens group reports[22] that for Mg impurities in Al,

$$T_{\text{max}} \propto \rho_0^{1/5}, \tag{6.3}$$

until for sufficiently large ρ_0, the hump is washed out. It is seen that these results are reproduced by the calculation. Another feature[1] of the data, and of the calculation, is that for sufficiently high temperatures, the values for $\Delta(T)/\rho_0$ approach a constant. The constant varies somewhat with ρ_0, but for each sample the constant lies in the range 0.1–0.2. This feature is also present for other alloy systems. Note that the observed temperature dependence and the ρ_0 dependence of the hump are reproduced by the same theory that accounts for the low-temperature DMR. In particular, the Kagan-Zhernov interference terms $\Delta\rho_{\text{int}}(T)$ contribute but little to $\Delta(T)/\rho_0$, except at higher temperatures and for larger values of ρ_0; they certainly do not produce the hump, as has sometimes been suggested. In fact, for the most impure sample, the effect of the contribution of $\Delta\rho_{\text{int}}(T)$ is to wash out the hump, rather than to produce it.

In spite of the rather close agreement between the calculation and the data, as indicated by Figs. 3–5, one should not form the impression that the present theory is correct to the last percentage point. This is most certainly not the case. We are interested in obtaining calculated values for $\Delta\rho(T)$ that are accurate to about 10%. A more

accurate calculation would require a number of refinements to the theory that would significantly complicate the analysis, as well as the numerical calculations. These refinements include (i) inclusion of the energy dependence of $\phi_{ph}(\vec{K})$, (ii) an improved expression for $\hat{P}_{imp}$, (iii) a more realistic phonon spectrum and (iv) a more accurate representation of the pseudo-wave-functions and of the Fermi surface. We shall briefly discuss in turn each of these improvements to the theory.

The approximate functional form chosen for $\phi_{ph}(\vec{K})$, given by (3.1), includes the angular dependence of $\phi_{ph}(\vec{K})$, but not its energy dependence. The reduction in $\Delta\rho(T)$ due to the energy dependence of $\phi_{ph}(\vec{K})$ is expected[54] to be small for polyvalent and noble metals. An explicit calculation has recently been carried out[54] for Al in the dirty limit, and it was found that $\Delta\rho(T)$ is reduced by about 10%, the magnitude of the reduction depending on the temperature under consideration.

The expression for $\hat{P}_{imp}$ that we used is approximate in several respects. No account was taken of lattice distortion.[40] Moreover, the pseudopotential representation of the screened electron-ion interaction matrix elements, based on a single empirical parameter, may not be adequate for electron-impurity scattering. Indeed, one should properly rely on a full phase-shift analysis,[35] rather than using the Born approximation to calculate the transition probability for electron-impurity scattering. (It should be emphasized that these remarks do *not* apply to electron-phonon scattering, for which the resistivity integral is dominated at low temperatures by the pseudopotential matrix elements evaluated at the reciprocal-lattice vectors, a quantity directly measured[31] in the de Haas–van Alphen experiment. Moreover, the Born approximation is certainly valid[35] for the weak electron-phonon interaction.) The error resulting from these approximations to $\hat{P}_{imp}$ is hard to determine accurately, but 10% is the right order of magnitude.

The true phonon spectrum differs from our assumed spectrum in two respects. We neglected dispersion, assuming that $\omega_\lambda(\vec{q})$ is linear in q for all q, and we neglected the angular dependence of the velocity of sound. For low temperatures, for which only low-q phonons enter the calculation, the neglect of dispersion is justified, but at higher temperatures, say $T > 40$ K ($\frac{1}{10}$ of the Debye temperature), phonon dispersion should be included. Regarding the neglect of the angular dependence of $\omega_\lambda(\vec{q})$, this is not serious, except at very low temperatures, because of the near isotropy of the true phonon spectrum of Al. Numerical tests that we have carried out indicate that the resulting error in the resistivity does not exceed a few percent.

The piecewise 2-OPW approximation that we used throughout for the pseudo-wave-functions and the Fermi surface is quite accurate. We have confirmed that the artificial discontinuities that it introduces into the Fermi surface do not affect $\Delta\rho(T)$ by more than 1–2% at any temperature. However, there are certain regions of the Fermi surface for which the electron-phonon scattering matrix elements require three or even four plane waves for highly accurate values of $\Delta\rho(T)$. This is particularly true at very low temperatures. In fact, for $T \lesssim 2$ K ($\frac{1}{200}$ of the Debye temperature), the piecewise 2-OPW approximation probably leads to quite serious errors in $\Delta\rho(T)$. However, for the temperatures that we consider here, the piecewise 2-OPW approximation is accurate to a few percent.

The above list of possible improvements to the theory is by no means exhaustive. Each item on this list implies an error in $\Delta\rho(T)$ of ~5–10%. Even taking into account the inevitable partial cancellation of errors, their cumulative effect probably leads to a rms error of about 10%. Indeed, the agreement between theory and experiment shown in Figs. 3–5 is really somewhat better than would have been expected. Therefore it seems pointless to expend the considerable effort required to include some of the above improvements in the theory, if one is not ready to include them all. We are here primarily interested in the simplest realistic calculation of $\Delta\rho(T)$ for Al that includes all physical effects associated with dramatic low-temperature anisotropy of the electron-phonon scattering probability and the important multiple-OPW character of the electron wave functions, of the Fermi surface and of the electron velocities. It should be emphasized that failure to include all these effects in the calculation of $\Delta\rho(T)$ may lead to gross errors at low temperatures, ranging from a factor of 2–3 to more than an order of magnitude. By contrast, it is our goal to show that if one includes all these properties of the polyvalent metal in a consistent manner, then one will faithfully reproduce all aspects of the $\Delta\rho(T)$ data. In particular, there is no need whatsoever to introduce *ad hoc* assumptions to account for the resistivity data. Figures 3–5 testify to the extent that we have achieved this goal.

VII. INTERFERENCE TERMS

The calculation of $\Delta\rho(T)$ described thus far is based on the approximation that one writes the total scattering operator $\hat{P}_{tot}$ as the sum of the electron-phonon scattering operator $\hat{P}_{ph}$ and the

electron-impurity scattering operator $\hat{P}_{imp}$, as given in (2.2). We now remove this approximation by including explicitly the contribution to $\Delta\rho(T)$ arising from the "interference" scattering operator $\hat{P}_{int}$, which takes into account the coupling (or "interference") between the transition probabilities for electron-phonon scattering and for electron-impurity scattering. The operator $\hat{P}_{int}$ gives rise to several terms, as first discussed by Kagan and Zhernov.[53] These terms are collectively called the interference terms and will be denoted by $\Delta\rho_{int}(T)$. Over the last few years, the explicit calculation[55-59] of $\Delta\rho_{int}(T)$ has been carried out for several metals at various levels of approximation. The most detailed work is that of Kus, Carbotte, and co-workers, who calculated $\Delta\rho_{int}(T)$ for sodium,[57] potassium,[57] lithium,[58] and aluminum.[59] Thus, the formalism for calculating $\Delta\rho_{int}(T)$ is by now well established.

An important conclusion to be drawn from these studies[56-59] is that the usual idealized-model calculations (spherical Fermi surface, single plane waves, approximate electron-phonon scattering integral, etc.) do not yield quantitatively reliable values for $\Delta\rho_{int}(T)$. Therefore, in the absence of values for $\Delta\rho_{int}(T)$ for Al that are based on a realistic description of the metal, we carried out the calculation of $\Delta\rho_{int}(T)$ based on the representation of Al that is given in Sec. IV. It emerged from our study that of the various terms that contribute to $\Delta\rho_{int}(T)$, only two are important for the temperature range we are considering. These are the change in the electron-phonon resistivity due to the fact that the vibrating lattice is altered by the occasional presence of a substitutional impurity in place of the host ion, to be denoted by $\Delta\rho_{int}^{(1)}(T)$, and the change in the residual resistivity due to the fact that the impurities are vibrating along with the lattice, to be denoted by $\Delta\rho_{int}^{(2)}(T)$. The physical origin of these two terms has been lucidly discussed by Bass.[1] We remark only that $\Delta\rho_{int}^{(1)}(T)$ and $\Delta\rho_{int}^{(2)}(T)$ correspond to coherent and incoherent inelastic scattering, respectively. The 2-OPW expressions for these terms are

$$\Delta\rho_{int}^{(1)}(T)=\frac{c\Omega_0}{16\pi^5\hbar M k_B T}\int\int\left(\frac{dS(\vec{K}_1)}{v(\vec{K}_1)}\right)\left(\frac{dS(\vec{K}_2)}{v(\vec{K}_2)}\right)[\Phi(\vec{K}_2)-\Phi(\vec{K}_1)]^2\sum_\lambda\frac{S'_\lambda(\vec{K}_1,\vec{K}_2)S_\lambda(\vec{K}_1,\vec{K}_2)}{F(\omega_{\vec{q}\lambda};T)} \tag{7.1}$$

$$\Delta\rho_{int}^{(2)}(T)=\frac{c\Omega_0}{32\pi^5\hbar M k_B T}\int\int\left(\frac{dS(\vec{K}_1)}{v(\vec{K}_1)}\right)\left(\frac{dS(\vec{K}_2)}{v(\vec{K}_2)}\right)[\Phi(\vec{K}_2)-\Phi(\vec{K}_1)]^2(\vec{K}_2-\vec{K}_1)^2|\langle\psi_{\vec{K}_1}|\Delta\hat{W}|\psi_{\vec{K}_2}\rangle|^2\frac{\Omega_0}{24\pi^3}\sum_\lambda\int\frac{d^3q}{F(\omega_{\vec{q}\lambda};T)}, \tag{7.2}$$

where the impurity concentration c is related to ρ_0 through (2.10) in the standard way,[40] the primed function $S'_\lambda(\vec{K}_1,\vec{K}_2)$ is the same as the unprimed function $S_\lambda(\vec{K}_1,\vec{K}_2)$, given by (5.5), except that $w(k)$ is everywhere replaced by $\Delta w(k)$, given by (5.9), and the temperature-dependent denominator $F(\omega_{\vec{q}\lambda};T)$ is defined by (2.9). In (7.2), the integral over $\vec{q}$ is taken over the first Brillouin zone.

A few comments are in order concerning (7.1) and (7.2). We have included the Debye-Waller factor but not the mass-change correction, which has been shown[59] to make only a small contribution to $\Delta\rho_{int}(T)$ for Al for the temperature range under consideration here. However, for higher temperatures approaching the Debye temperature, the mass-change correction is no longer small[59] and should be included. The form factor of the substitutional impurity $\Delta w(k)$ can be either positive or negative, and hence $\Delta\rho_{int}^{(1)}(T)$ can be positive or negative, depending on the type of impurity present and on the weighting of the integrand at differing temperatures. In particular, for a vacancy, for which $\Delta w(k)=-w(k)$, it follows that $\Delta\rho_{int}^{(1)}(T)$ will be negative for all temperatures. The possibility that $\Delta\rho_{int}(T)$ may become negative at higher temperatures for certain impurities was first pointed out by Bhatia and Gupta.[55] Turning now to $\Delta\rho_{int}^{(2)}(T)$, the integral over q is just the phonon specific-heat integral at low temperatures. Therefore including the factor T^{-1} multiplying the integral yields that $\Delta\rho_{int}^{(2)}(T)\propto T^2$ at very low temperatures, as first pointed out by Kagan and Zhernov.[53,56]

We have evaluated the integrals (7.1) and (7.2) for various substitutional impurities in Al. Magnesium impurity is chosen to illustrate the results in Fig. 6 because Mg was the impurity present in the samples whose $\Delta(T)$ is given in Fig. 5. The results for $\Delta\rho_{int}(T)/\Delta\rho(T)$ are given by the solid curve (vertical scale on left-hand side) in Fig. 6 for $\rho_0=10$ $\mu\Omega$ cm, corresponding to a very impure sample. This value of ρ_0 is near the largest value of ρ_0 that one is able to obtain experimentally, and it corresponds to the dirty limit even for temperatures as high as 100 K.

From the solid curve, one sees that $\Delta\rho_{int}(T)/\Delta\rho(T)$ decreases rapidly with temperature, dropping from about 30% at 14 K to about 5% at 40 K. However, this does not imply that $\Delta\rho_{int}(T)$ is most

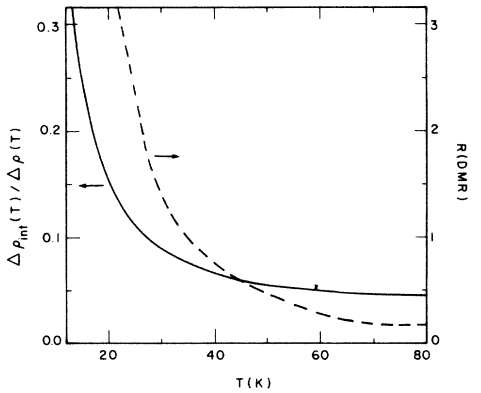

FIG. 6. Calculated temperature dependences of the ratio $\Delta\rho_{int}(T)/\Delta\rho(T)$ and of the magnitude of the DMR, denoted by R(DMR) and defined by Eq. (7.3). Note that the left-hand scale for $\Delta\rho_{int}(T)/\Delta\rho(T)$ is a factor of 10 smaller than the right-hand scale for R(DMR).

important at low temperatures. In fact, exactly the opposite is the case. Only at higher temperatures does $\Delta\rho_{int}(T)$ contribute significantly to the DMR. The reason for this is best seen by examining the temperature dependence of the magnitude of the DMR [calculated without $\Delta\rho_{int}(T)$], denoted by R(DMR) and defined by

$$R(\mathrm{DMR}) = \frac{[\Delta\rho(T)]_{\mathrm{dirty}}}{[\Delta\rho(T)]_{\mathrm{pure}}} - 1, \tag{7.3}$$

where the unity has been subtracted to insure that R(DMR) = 0 when there are no DMR. The calculated values for R(DMR) are given by the dashed curve (vertical scale on right-hand side) in Fig. 6. Note in particular that the scale of R(DMR) is a factor of 10 larger than the scale of $\Delta\rho_{int}(T)/\Delta\rho(T)$.

At low temperatures, say 14 K, the 30% contribution of $\Delta\rho_{int}(T)$ to $\Delta\rho(T)$ is a very much smaller effect than the very large DMR, i.e., the factor-of-6 increase in $\Delta\rho(T)$ in going from the pure to the dirty limit. By contrast, at higher temperatures, say 77 K, the 5% contribution of $\Delta\rho_{int}(T)$ to $\Delta\rho(T)$ is the same order of magnitude as the 20% DMR. Accordingly, as is clear from Fig. 5, it is at high temperatures that $\Delta\rho_{int}(T)$ contributes measureably to $\Delta(T)$ for larger-ρ_0 samples, whereas at lower temperatures (<50 K), the effect of $\Delta\rho_{int}(T)$ on $\Delta(T)$ is negligible for all samples.

In summary, at each temperature, the importance of $\Delta\rho_{int}(T)$ is determined by comparing $\Delta\rho_{int}(T)/\Delta\rho(T)$ to the magnitude of the DMR. The calculation shows that only at higher temperatures and only for the dirtier samples is the ratio $\Delta\rho_{int}(T)/\Delta\rho(T)R$(DMR) not completely negligible.

From the preceding discussion, one may conclude that the contribution of $\Delta\rho_{int}(T)$ is not especially important for calculating the general properties of the DMR for polyvalent and noble metals. Nevertheless, the role of $\Delta\rho_{int}(T)$ has assumed an unexpected importance due to the issue of "saturation." Without $\Delta\rho_{int}(T)$, the values for $\Delta\rho(T)$ are predicted to saturate at large ρ_0, whereas the data continue to rise with increasing ρ_0. This observed lack of saturation has sometimes been used[2] as "evidence" for discarding entirely the present theory of the DMR that is based on the isotropization of the electron distribution function $\Phi(\vec{K})$ with increasing electron-impurity scattering. However, one sees that it is possible to explain quantitatively the lack of saturation of $\Delta\rho(T)$ at large ρ_0 on the basis of $\Delta\rho_{int}(T)$.

VIII. PREVIOUS WORK

The calculation of $\Delta\rho(T)$ at low temperatures for polyvalent metals in general and for Al in particular has been the subject of considerable theoretical interest for many years. We shall not, of course, attempt to give a complete discussion of all the many important papers dealing with the low-temperature calculations of $\Delta\rho(T)$. Our discussion will necessarily be restricted to those papers that are directly related to the present calculation. These papers fall naturally into two groups. One group of papers deals with the calculation of the DMR for polyvalent metals and the second group deals with the low-temperature calculation of $\Delta\rho(T)$ in what we have called the dirty limit, without calculating the DMR.

We first discuss those papers that deal with the calculation of the DMR, the major subject of the present work. Of particular interest is the analysis by Trofimenkoff and Bhatia[36] (TB) of the DMR for a polyvalent metal based on an *exact* solution of the Boltzmann equation for an idealized model of the electron-phonon scattering transition probability. Although the model assumed for the scattering is not directly applicable to any real metal, nevertheless, the analysis is extremely valuable because TB obtain, without approximation, two crucial results whose importance can hardly be overemphasized for an understanding of the low-temperature DMR. First, in the pure limit, the low-temperature electron distribution function $\Phi(\vec{K})$ is dramatically reduced in the vicinity of each of the intersections of the Fermi surface and the Brillouin-zone boundaries. Second, in the pure limit, the umklapp-scattering term ρ_U is negligible compared to the normal-scattering term ρ_N, even though the reverse is true for the dirty limit. To be specific, for the model parameters chosen by TB, the umklapp-

to-normal scattering ratio ρ_U/ρ_N equals 10 in the dirty limit, but only 0.005 in the pure limit, a drop of 3 orders of magnitude. It is clear that any calculation that does not yield these two crucial results cannot possibly lead to quantitatively reliable values for the DMR.

In spite of the importance of the TB analysis, one cannot of course compare $\Delta\rho_{\text{exp}}(T)$ for a specific metal with $\Delta\rho_{\text{calc}}(T)$ obtained from an idealized model for the electron-phonon scattering transition probability. Therefore, we have combined in the present work an accurate real-metal representation of the electron-phonon scattering transition probability for Al with a variational solution to the Boltzmann equation that explicitly includes the correct behavior of the electron distribution function. The form chosen for $\Phi(\vec{K})$ in the pure limit, given by (3.1), contains the factor $[v(\vec{K})/v_F]^n$, where n is determined by the variational theorem. For large n, one automatically obtains the required reduction in $\Phi(\vec{K})$ near the intersection of the Fermi surface and the Brillouin-zone boundaries. As a result, our calculation yields that for low temperatures, the umklapp-to-normal scattering ratio ρ_U/ρ_N varies from being large in the dirty limit (= 8.1 at 10 K) to being very small in the pure limit (= 0.12 at 10 K). The reduction of ρ_U/ρ_N from $\gg 1$ to $\ll 1$ is central to obtaining the correct low-temperature values of the DMR, as TB so clearly showed. Indeed, all aspects of our results for $\Delta\rho(T)$ are completely consistent with the exact results of the TB analysis of the model system.

Other important previous calculations of the DMR include those of Ehrlich,[60] Schotte and Schotte,[61] Kagan and Zhernov,[56] Dosdale and Morgan,[62] Kus and Carbotte,[59] and Gorham-Bergeron and Dworin.[37] The Ehrlich[60] and Schotte and Schotte[61] calculation of the DMR are based on a generalization of the Klemens-Jackson[63] diffusion-equation approach to $\Delta\rho(T)$ to include impurity scattering and they will be discussed together with the Klemens-Jackson calculation. The other four papers[37,56,59,62] present Boltzmann-equation calculations of the DMR, with various levels of approximation used to describe the electron-phonon scattering transition probability of Al and the electron distribution function. All these calculations[37,56,59-62] obtain qualitatively correct results in that they find the required reduction of $\Phi(\vec{K})$ in the pure limit near the Brillouin-zone boundaries and the resulting marked increase in $\Delta\rho(T)$ in going from the pure limit to the dirty limit. However, in none of these calculations is there proper appreciation of the importance of normal scattering. In each case, ρ_N turns out to be negligible even in the pure limit because of the inappropriate use of 1-OPW electron wave functions and/or the use of an incorrect electron distribution function and/or the explicit (incorrect) assumption that ρ_N does not contribute to the DMR. Nevertheless, this shortcoming should not obscure the fact that each of these papers[37,56,59-62] makes an important contribution to our understanding of the low-temperature DMR for Al.

We now turn to the group of papers which deal with the low-temperature calculation of $\Delta\rho(T)$ in the dirty limit only. These calculations are relevant in that they include, at least partially, the multiple-OPW character of the electron wave functions, of the Fermi surface, of the electron velocities, of the electron-phonon scattering transition probability, etc. The pioneering calculation of $\Delta\rho(T)$ for Al is surely the 1967 calculation of Pytte,[64] who used a 2-OPW electron wave function and included the Fermi-surface distortions from sphericity that had shortly before been determined by Ashcroft.[31] This was the best calculation at that time. However, it is now recognized that the resulting $\Delta\rho(T)$ is not accurate at low temperatures because of certain approximations introduced to facilitate the angular integrations, which prevent a correct treatment of the crucial small-q region of the resistivity integrals, and because $\Phi(\vec{K})$ was taken to be proportional to $\vec{K}\cdot\vec{E}$ instead of $\vec{v}(\vec{K})\cdot\vec{E}$. Improved versions of the Pytte[64] calculation subsequently appeared, such as that of Truant and Carbotte,[65] but still based on $\Phi(\vec{K}) \propto \vec{K}\cdot\vec{E}$. A major advance in the calculation of $\Delta\rho(T)$ for Al was the detailed study of Lawrence and Wilkins,[66] whose completely realistic description of Al also includes the correct dirty-limit electron distribution function, $\Phi(\vec{K}) \propto \vec{v}(\vec{K})\cdot\vec{E}$, and a correct calculation of the normal scattering contribution to $\Delta\rho(T)$. As a result, meaningful results were obtained for $\Delta\rho(T)$ for Al, unmarred by the commonly-made approximations. The Lawrence-Wilkins calculation has recently been generalized by Leung *et al.*[67] by the use of 15 plane waves to describe the electron pseudo-wave-functions. The present dirty-limit calculation of $\Delta\rho(T)$ is most closely related to the Lawrence-Wilkins calculation,[66] except that we have included certain important refinements, such as the piecewise 2-OPW framework, which are of particular significance at the lowest temperatures, where the numerical work is especially treacherous.

An entirely different approach to the calculation of $\Delta\rho(T)$ for polyvalent metals is that of Klemens and Jackson,[63] who showed that under certain assumptions, the Boltzmann equation can be transformed into a diffusion equation. Owing to electron-phonon scattering, the electrons move over

the Fermi surface, assumed spherical, in random steps sufficiently small that the process can be regarded as taking place by diffusion. The resulting diffusion equation is solved to yield $\Delta\rho(T)$. Including impurity scattering, as was done by Ehrlich[60] and by Schotte and Schotte,[61] permits an explicit calculation of the DMR. However, the Klemens-Jackson-Ehrlich-Schotte-Schotte approach is not an alternative to the present calculation because the "diffusion coefficient" that results from electron-phonon scattering is not calculated. Rather, it is treated as an empirical parameter with an assumed temperature dependence. Moreover, as with the other calculations of the DMR, the important contribution to the DMR of the normal-scattering term was not properly taken into account.

IX. SUMMARY

A detailed analysis has been presented of the low-temperature behavior of the electrical resistivity of dilute alloys of Al. Our principal results are the following:

(i) A new electron distribution function has been introduced for electron-phonon scattering which takes explicit account of the enormous anisotropy at low temperatures of the transition probability for electron-phonon scattering. Based on this new distribution function, the variational method is employed to solve the Boltzmann equation and to obtain the resistivity.

(ii) The piecewise 2-OPW framework is introduced and shown to yield an accurate description of the relevant properties of Al. This multiple-OPW description of Al is used for evaluating the resistivity integrals and leads to accurate values for the calculated resistivity.

(iii) In the pure limit, the normal-scattering term is found to be much larger than the umklapp-scattering term. This surprising result is in precise agreement with the exact model calculation of Trofimenkoff and Bhatia.

(iv) The dependence of the resistivity on impurity concentration is calculated for various values of temperature, and the temperature dependence of the resistivity is calculated for various values of impurity concentration. In each case, excellent quantitative agreement is obtained with the experimental data for Al.

(v) The interference terms are explicitly calculated within the piecewise 2-OPW framework and are shown to be small in most cases. However, in the dirty limit, the interference terms are important and are shown to be responsible for the observed lack of saturation of the resistivity as a function of impurity concentration.

(vi) The observed "humps" in the resistivity-versus-temperature curves are accurately reproduced by the calculation. In particular, the humps are shown to be unrelated to the interference terms.

ACKNOWLEDGMENTS

We wish to thank Dr. E. Rocofyllou for sending us a list of all the detailed resistivity data for Al measured by her and her colleagues at the Democritos Nuclear Research Center of Athens. We also gratefully acknowledge the financial support provided by the Israel Commission for Basic Research.

[1]J. Bass, Adv. Phys. 21, 431 (1972).
[2]M. R. Cimberle, G. Bobel, and C. Rizzuto, Adv. Phys. 23, 699 (1974).
[3]R. Reich, Ph.D. thesis, University of Paris, 1965 (unpublished).
[4]A. D. Caplin and C. Rizzuto, J. Phys. C 1, L117 (1970).
[5]R. S. Seth and S. B. Woods, Phys. Rev. B 2, 2961 (1970).
[6]J. W. Ekin and B. W. Maxfield, Phys. Rev. B 2, 4805 (1970).
[7]A. D. Caplin and C. Rizzuto, Aust. J. Phys. 24, 309 (1971).
[8]J. W. Ekin, Ph.D. thesis, Cornell University, Ithaca, New York, 1971 (unpublished).
[9]I. A. Campbell, A. D. Caplin, and C. Rizzuto, Phys. Rev. Lett. 26, 239 (1971).
[10]F. R. Fickett, Phys. Rev. B 3, 1941 (1971).
[11]R. Krsnik, A. D. Caplin, and C. Rizzuto, Solid State Commun. 12, 891 (1973).
[12]S. Senoussi and I. A. Campbell, J. Phys. F 3, L19 (1973).
[13]T. Kino, T. Endo, and S. Kawato, J. Phys. Soc. Jpn. 36, 698 (1974).
[14]N. Kontoleon, K. Papathanasopoulos, K. Chountas, and C. Papastaikoudis, J. Phys. F 4, 2109 (1974).
[15]C. Papastaikoudis and K. Papathanasopoulos, Solid State Commun. 16, 1083 (1975).
[16]C. Papastaikoudis, N. Kontoleon, K. Papathanasopoulos, and P. Andronikos, Phys. Rev. B 11, 2077 (1975).
[17]R. W. Klaffsky, N. S. Mohan, and D. H. Damon, J. Phys. Chem. Solids 36, 1147 (1975).
[18]S. Kawato and T. Kino, J. Phys. Soc. Jpn. 39, 684 (1975).
[19]J. A. Rowlands and S. B. Woods, J. Phys. F 5, L100 (1975).
[20]E. Babic, R. Krsnik, and M. Ocko, J. Phys. F 6, 73 (1976).
[21]C. Papastaikoudis and E. Rocofyllou, Solid State Commun. 18, 1161 (1976).
[22]K. Papathanasopoulos and E. Rocofyllou, Solid State Commun. 19, 665 (1976).

[23]C. Papastaikoudis, K. Papathanasopoulos, and E. Rocofyllou, J. Phys. F 6, 409 (1976).
[24]Y. Fujita and T. Ohtsuka, J. Low Temp. Phys. 29, 333 (1977).
[25]M. N. Klopkin, G. K. Panova, and B. N. Samoilov, Zh. Eksp. Teor. Fiz. 72, 550 (1977) [Sov. Phys.–JETP 45, 287 (1977)].
[26]Y. Fujita and Y. Fukai, and K. Watanabe, J. Phys. F 7, L175 (1977).
[27]J. C. Garland and D. J. van Harlingen, J. Phys. F 8, 117 (1978).
[28]Y. Fujita and Y. Fukai, J. Phys. F 8, 1209 (1978).
[29]J. A. Rowlands and S. B. Woods, J. Phys. F 8, 1929 (1978).
[30]C. Papastaikoudis, E. Thanou, D. Tsamakis, and W. Tselfes, J. Low Temp. Phys. 34, 429 (1979).
[31]N. W. Ashcroft, Philos. Mag. 8, 2055 (1963).
[32]G. Gilat and R. M. Nicklow, Phys. Rev. 143, 487 (1966).
[33]E. R. Cowley, Can. J. Phys. 52, 1714 (1974).
[34]M. Kaveh and N. Wiser, preceding paper, Phys. Rev. B 21, 2278 (1980).
[35]J. M. Ziman, *Electrons and Phonons* (Clarendon, Oxford, 1960).
[36]P. N. Trokimenkoff and A. B. Bhatia, J. Phys. F 4, 1719 (1974).
[37]E. Gorham-Bergeron and L. Dworin, Phys. Rev. B 11, 4859 (1975).
[38]Y. Bergman, M. Kaveh, and N. Wiser, Phys. Rev. Lett. 32, 606 (1974).
[39]See, for example, L. I. Schiff, *Quantum Mechanics*, 3rd ed. (McGraw-Hill, New York, 1968), Sec. 32.
[40]R. S. Sorbello, Solid State Commun. 12, 287 (1973).
[41]See, for example, C. Kittel, *Introduction to Solid State Physics*, 3rd ed. (Wiley, New York, 1966), Chaps. 4 and 9.
[42]B. J. Austin, V. Heine, and L. J. Sham, Phys. Rev. 127, 276 (1962).
[43]F. Herman and S. Skillman, *Atomic Structure Calculations* (Prentice-Hall, Englewood Cliffs, N.J., 1963).
[44]M. Kaveh and N. Wiser, Phys. Rev. B 9, 4053 (1974).
[45]N. Wiser and A. J. Greenfield, Adv. At. Mol. Phys. 7, 363 (1971).
[46]N. W. Ashcroft, Phys. Lett. 23, 48 (1966).
[47]C. R. Leavens and R. Taylor, J. Phys. F 8, 1969 (1978).
[48]A. J. Greenfield and N. Wiser, J. Phys. F 5, 1289 (1975).
[49]L. J. Sham and J. M. Ziman, Solid State Phys. 15, 221 (1963), Sec. 11.
[50]Y. Fukai, Phys. Rev. 186, 697 (1969).
[51]J. Brown, J. Phys. F 7, 1283 (1977).
[52]M. Kaveh and N. Wiser, J. Phys. F (to be published).
[53]Y. Kagan and A. P. Zhernov, Zh. Eksp. Teor. Fiz. 50, 1107 (1966) [Sov. Phys.–JETP 23, 737 (1966)].
[54]A. Bergmann, M. Kaveh, and N. Wiser, J. Phys. (Paris) 39, C6-1044 (1978) (Proceedings of the XV International Conference on Low Temperature Physics).
[55]A. B. Bhatia and O. P. Gupta, Phys. Lett. 29A, 358 (1969).
[56]Y. Kagan and A. P. Zhernov, Zh. Eksp. Teor. Fiz. 60, 1832 (1971) [Sov. Phys.–JETP 33, 990 (1971)]
[57]F. W. Kus, B. A. White, J. Mason, and J. P. Carbotte, Can. J. Phys. 52, 1511 (1974).
[58]F. W. Kus, J. P. Carbotte, and D. W. Taylor, Phys. Rev. B 12, 1227 (1975).
[59]F. W. Kus and J. P. Carbotte, Can. J. Phys. 53, 1693 (1975).
[60]A. C. Ehrlich, Phys. Rev. B 1, 4537 (1970).
[61]D. Schotte and U. Schotte, Solid State Commun. 10, 131 (1972).
[62]T. Dosdale and G. J. Morgan, J. Phys. F 4, 402 (1974).
[63]P. G. Klemens and J. L. Jackson, Physica 30, 2031 (1964).
[64]E. Pytte, J. Phys. Chem. Solids 28, 93 (1967).
[65]P. T. Truant and J. P. Carbotte, Can. J. Phys. 52, 618 (1974).
[66]W. E. Lawrence and J. W. Wilkins, Phys. Rev. B 6, 4466 (1972).
[67]H. K. Leung, F. W. Kus, N. McKay, and J. P. Carbotte, Phys. Rev. B 16, 4358 (1977).